Domain-wall relaxation near the disorder transition of Bloch walls in Sr hexaferrite

M. Hartl-Malang and J. Kötzler
Institut für Angewandte Physik, Universität Hamburg, D-20355 Hamburg, Germany

D.A. Garanin
I. Institut für Theoretische Physik Universitat, Hamburg, D-20355 Hamburg, Germany
(Received 26 October 1994)

By measuring the linear ac susceptibility of single crystals of $SrFe_{12}O_{19}$ between 10 Hz and 20 MHz, the domain-wall dynamics have been investigated near the continuous phase transition from Bloch to linear walls at $T^* \approx 0.99T_C$. There the kinetic coefficient of the wall relaxation L_w has a deep minimum, the essential features of which indicate the presence of strong, two-dimensional Ising-like fluctuations of the order parameter of the Bloch walls. Magnetic fields, applied transverse to the easy **c** axis, increase L_w in almost quantitative agreement with predictions of the Landau-Lifshitz-Bloch approach for the mean-field region away from T^*. Effects of fluctuations in the critical region of the disordered phase remain unexplained.

I. INTRODUCTION

As a unique feature of uniaxial ferromagnets and ferrimagnets, Bulaevskii and Ginzburg[1,2] predicted the continuous disappearance of Bloch domain walls (DW's) at a temperature T^* below the Curie point T_C. The existence of this phase transition, characterized by the so-called Bloch-wall (BW) order parameter [$m_B \propto M_y(x = 0)$], which is given by the in-plane magnetization component perpendicular to the easy (z) axis in the wall center ($x = 0$), arises from the fact that the transverse susceptibility $\chi_\perp$ of uniaxial magnets remains constant at and below T_C. This implies that at an elevated temperature $T^* < T_C$, the density of the anisotropy energy, $2M_s^2/\chi_\perp$ (M_s = spontaneous magnetization), associated with the BW order parameter exceeds the energy density of the longitudinal component, $M_s^2/2\chi_z$, which rapidly diminishes near T_C due to the fluctuations of the bulk order parameter M_z. Within the mean-field approach (MFA),[1,2] the order parameter of the BW, $m_B \equiv M_y(x = 0)/M_s$, continuously disappears,

$$m_B^{\mathrm{MF}}(\tau < 1) = (1 - \tau)^{1/2}, \quad m_B(\tau > 1) = 0, \qquad (1.1)$$

at T^*_{MF}, where the ratio between these two energy densities,

$$4\chi_z(T)/\chi_\perp = \tau(T), \qquad (1.2)$$

reaches $\tau(T^*_{\mathrm{MF}}) = 1$. This MF result suggests considering τ as the temperature variable of this transition. Above T^*_{MF}, the transverse component of the wall magnetization disappears, $M_y(x) = 0$, and the linear-wall (LW) structure becomes stable.

Evidence for LW's has been obtained experimentally by investigations of the temperature, magnetic field, and sample-size variations of the relaxation rate of the domain walls, Γ_w, in the uniaxial ferromagnets $GdCl_3$ (Ref. 3) and $LiTbF_4$.[4] As the most pronounced feature we mention here the critical speeding up, $\Gamma_w(T \to T_C) \propto (T_C - T)^{-z}$, the critical exponent $z = 0.75(5)$ and the magnitude of which could almost quantitatively be explained assuming the linear structure of the DW's. The key property of the LW's causing the rapid increase of the relaxation rate towards T_C is the growing number of wall spins determined by the width of the LW's, $\delta_L = 2\xi_z$,[1] i.e., by the correlation length of the bulk magnetization diverging at T_C. Due to the low Curie temperatures $T_C = 2.21$ K and 2.87 K of $GdCl_3$ (Ref. 3) and $LiTbF_4$,[4] respectively, and because of their moderate anisotropies, their wall reconstruction temperatures are so small ($T^*_{\mathrm{MF}} \ll T_C$) that an indication for a change of the DW structure was not seen.

More recent investigations of the domain-wall relaxation rates Γ_w in the ferrimagnets $BaFe_{12}O_{19}$ (Ref. 5) and $SrFe_{12}O_{19}$,[6] however, revealed rather significant fingerprints of such a structural transition of the DW. Due to the large exchange energies in these materials (T_C = 740–750 K), one expects from Eq. (1.2) wall transition temperatures as high as $T^*_{\mathrm{MF}} = 0.996\,T_C$. Indeed, at temperatures $T^* \lesssim T^*_{\mathrm{MF}}$ deep minima of Γ_w were detected in both ferrimagnets. Below T^*, this variation of Γ_w could rather accurately be described using the so-called Landau-Lifshitz-Bloch (LLB) approach[7,8] and assuming a non-MFA behavior of the BW order parameter,[6]

$$m_B(\tau) = \left(1 - \frac{\tau}{\tau^*}\right)^{\beta} \quad (\tau < \tau^*). \qquad (1.3)$$

This analysis revealed an effective critical exponent $\beta = 0.08(1)$ far below the MFA value $\beta = 1/2$ and being even smaller than $\beta = 1/8$ of the two-dimensional (2D) Ising model. Moreover, the drastic shift of the transition temperature $\tau^* = 0.3$ from the MF value $\tau^*_{\mathrm{MF}} = 1$ predicted by Eq. (1.1) indicated the presence of strong fluctuations in the walls. For temperatures away from this transition region, the wall relaxation obeyed the MFA law, Eq. (1.1): For $\tau \gg 1$ pure LW behavior was observed while for $\tau \to 0$ the transition to the well-known limit, $\Gamma_w \sim (\gamma M_s)^2/L_\perp$, predicted by Landau and Lifshitz[9] for

circular BW's ($m_B = 1$) occurred. In the latter case Γ_w is determined by the small (spin-spin) correlation rate of the transverse magnetization components $L_\perp$, whereas at finite temperatures thermal fluctuations of the ferromagnetic order parameter give rise to a finite χ_z, which reduces m_B and hence produces an elliptical shape of the DW. The motion of these elliptical walls (EW's) implies a change of the modulus of $\mathbf{M}(x)$ involving the longitudinal ("spin-lattice") relaxation determined by the parameter L_z and leading to a reduction of the wall motion and damping frequency when T^* is approached from low temperatures.

Despite the success of the MFA in the limiting cases of LW's ($\tau \gg 1$) and of nearly BW's ($\tau \ll 1$) and of the highly critical law, Eq. (1.3), just below $T^*(\tau \lesssim 1)$, a number of questions about the nature of this transition remain open. One of the main problems is concerned with the universality class of this transition. Theoretical work by Lawrie and Lowe[10] argued that due to the one degree of freedom of the BW order parameter, $m_B \sim M_y(0)$, the two-dimensional Ising model should be the appropriate universality class in a vicinity of T^* where the correlation length of the BW order parameter ξ_B exeeds the width of the wall, δ, so that the correlations can be considered as two dimensional. As noted above, the fitted exponent $\beta = 0.08(1)$ is even smaller than the 2D Ising value, $\beta = 1/8$, and also the critical temperature variable $\tau^* \simeq 0.3$ is reduced by more than 50% from the MF temperature. Hence, the applicability of the 2D Ising model near the DW transition appears to be questionable, also since it discards other possible sources for fluctuations like the XY type and roughening of the walls. Another open problem is the behavior of Γ_w just above T^* where the data are significantly larger than those calculated within the MFA. This feature also suggests considering fluctuation effects not only on m_B itself but also for the width of the DW's on both sides of the transition.

Here we present further investigations of this DW transition aiming at a better understanding of the thermal nucleation and growth of the BW's. As before, our experimental access will be the wall dynamics, and here we study the influence of magnetic fields $H_\perp$ applied transverse to the easy axis of single $SrFe_{12}O_{19}$ crystals. Because $H_\perp$ couples to the BW order parameter, it may induce finite values for m_B already above T^*. Thus a significant increase of Γ_w is expected there,[8] while at the same time critical fluctuations of m_B should be suppressed. From this field dependence, a deeper insight into the critical properties of the wall transition is expected.

These effects of a transverse field will be contrasted to those of longitudinal fields, H_z, applied parallel to the easy axis. They do not couple to m_B because they are screened from the interior of the sample so that the wall mobility, $\mu_w \equiv v_w/\Delta H$, should not change. On the other hand, the gain in potential energy of the sample in H_z being balanced by the magnetostatic surface and the wall energies leads to an increase of the domain period and hence to a reduction of Γ_w; see, e.g., Ref. 3. These investigations as well as those of the effect of the sample thickness on Γ_w performed here should help to substantiate the micromagnetic assumptions as far as they are needed to interpret the Γ_w data obtained in zero and finite transverse fields near the structural transition of the DW's.

The experimental results comprising static and dynamic properties are presented in Sec. II. The general tools required for the discussion, i.e., the link between Γ_w and the wall moblity, the results of the LLB approach for μ_w, and the MFA results for the DW profile, are summarized in Sec. III. The first part of the discussion presented in Sec. IV is devoted to the wall dynamics in zero transverse fields, where we examine separately the influence of the sample thickness, of longitudinal fields, and of thermal fluctuations on Γ_w. We then discuss the effects of finite transverse fields based on the MFA for the wall profile to demonstrate where and how fluctuation effects on the wall dynamics become important. Section V provides a brief summary and our conclusions and is in particular intended to motivate further theoretical work on the interplay between thermal fluctuations of m_B, the width of the DW, and the dynamics near the reconstruction temperature. This will be necessary to fully understand the wall damping investigated here.

II. EXPERIMENTAL RESULTS

Near the Curie temperature of the hexagonal ferrite $SrFe_{12}O_{19}$, $T_C = 740.5$ K, the complex linear ac susceptibility $\chi(\omega) = \chi'(\omega) - i\chi''(\omega)$ has been measured between 10 Hz and 20 MHz parallel to the easy c axis of high quality single crystals.[11] Drifts of the background of the balanced mutual inductance connected to conventional lock-in detection were determined separately for each temperature scan. In the range of temperatures and fields investigated here, the sample response proved to be linear for excitation amplitudes near $H_{ac} \approx 0.7$ Oe. Figure 1 shows a scheme of the measuring system. In order to minimize changes in the sensitivity of the mutual inductance, Pt coils have been fixed on Al_2O_3-ceramic tubes by a ceramic cement having a similar thermal expansion coefficient. The Pt-100 temperature sensor is mounted next to the sample outside the primary coil, allowing a temperature resolution of approximately 5 mK at 740 K. The homemade oven is directly heated with a resistor element and has a temperature gradient of less than 0.05 K/cm across the sample. Using a high-reflectivity radiation shield, the outer diameter of the oven could be kept small enough to fit to either a solenoid or to a Helmholtz magnet with iron core providing the fields parallel or perpendicular to the c axis, respectively.

As an example, Fig. 2 shows the pronounced temperature variation of the dynamic susceptibility recorded at fixed frequency $f = 5$ kHz in fields up to 1.1 kOe applied parallel and perpendicular to the easy axis. For parallel fields, we have marked the temperatures T_D, where the spontaneous magnetization $M_s(T)$ reaches the value H_z/N_z and, therefore, the macroscopic internal field, $H_{z,i} = H_z - N_z M_z$, is expected to vanish due to the formation of domains below $T_D(H)$. Thus above T_D the response results from the domain-free sample, while be-

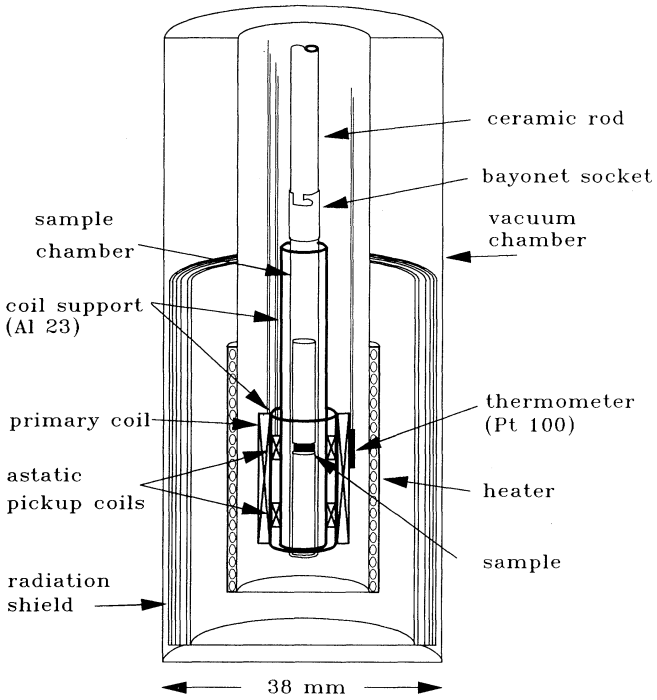

FIG. 1. Experimental setup to measure mutual inductances at temperatures up to 850 K.

low T_D the signal arises from the domain-wall dynamics of main concern here. On the other hand, small transverse fields applied here, $H_\perp < M_s/\chi_\perp$ do not destroy the domains which is consistent with the fact that the sharp peak of χ' at T_C remains unchanged. The main effect of $H_\perp$ is to shift the minimum of χ' below T_C to higher temperatures.

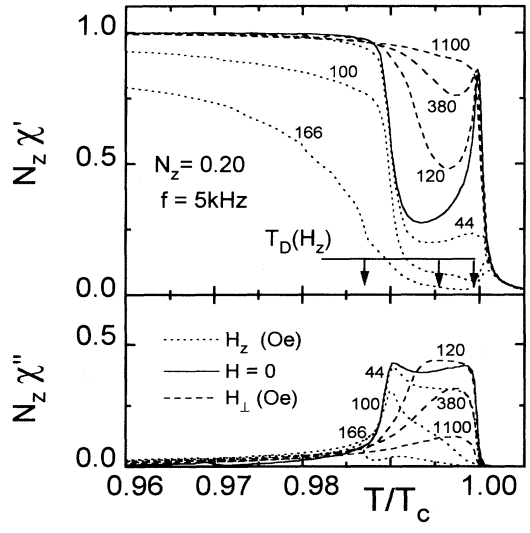

FIG. 2. Complex susceptiblity of a $SrFe_{12}O_{19}$ cylinder, with demagnetization coeffiecient $N = 0.20$ measured at constant frequency $f = 5$ kHz in different fields applied parallel and perpendicular to the easy c axis, respectively. Below T_D the internal field vanishes due to domain formation.

The dynamic behavior of the walls follows from the frequency dependence of χ' and χ'' displayed for temperatures below T_C in Fig. 3. Over a wide range of temperatures, the data can be described by one relaxation process, which for $\omega \to 0$ leads to the demagnetization plateau $\chi_w = N_z^{-1}$ and may therefore be related[12] to the relaxation of domain walls having a large internal susceptibility, $\chi_{w,i} \gg N_z^{-1}$. Near T_C, the dispersion exhibits an additional plateau indicating a second relaxation process, and dispersion and absorption can rather accurately be fitted to a sum of modified Debye functions,

$$\chi(\omega) = \frac{\chi_w - \chi_d}{1 + \left(\frac{i\omega}{\Gamma_w}\right)^{1-\alpha}} + \frac{\chi_d}{1 + \left(\frac{i\omega}{\Gamma_d}\right)^{1-\alpha'}}, \qquad (2.1)$$

where the relaxation rate Γ_w turns out to be much smaller than Γ_d. The slight deviation from the conventional Debye process is described by the small exponents α and α', which characterize distribution widths for Γ_w and Γ_d. The inset of Fig. 4 shows that α assumes a maximum near $T^* \approx 0.99\,T_C$. The resulting mean wall relaxation rates are depicted in Fig. 4 which demonstrates the completely different effects of the longitudinal and transverse fields on Γ_w between T_C and T^*: While H_z suppresses Γ_w in agreement with previous results on the low-temperature ferromagnet $GdCl_3$,[3] we here report an observation of the enhancement of Γ_w by a transverse applied field.

In order to discuss these central results for $\Gamma_w(T, \mathbf{H})$ in terms of the LLB approach, we have also determined the dc magnetization and susceptibilities. The longitudinal magnetizations measured by the $MPMS_2$ superconducting quantum interference device (SQUID) magnetometer (Quantum Design) are presented as modified Arrott plots in Fig. 5(a). For the fields and temperatures of interest here, they reveal the Curie temperature,

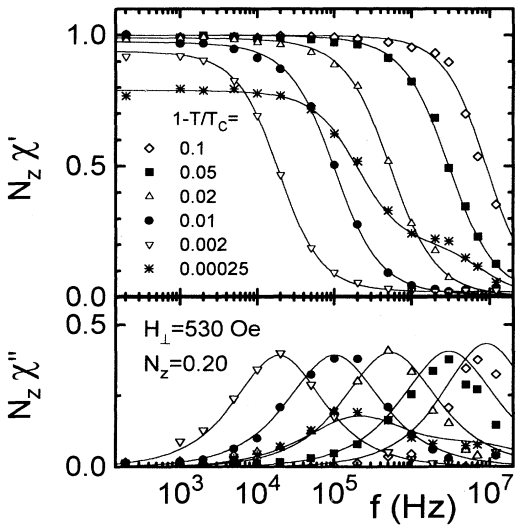

FIG. 3. Frequency dependence of dispersion and absorption in the field $H_\perp = 530$ Oe applied perpendicular to the c axis. Solid curves represent fits to the modified Debye function Eq. (2.1).

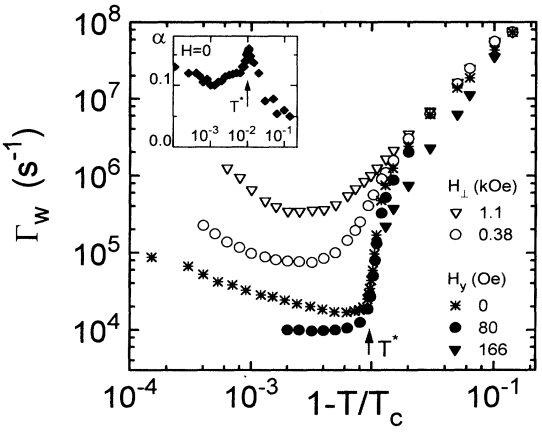

FIG. 4. Temperature variation of the wall relaxation rates Γ_w determined from Eq. (2.1) for different fields applied parallel and perpendicular to the easy c axis. The inset shows the temperature dependence of the deviation parameter α.

$T_C = 740.5(2)$ K, and the power laws for the zero-field susceptibility, $\chi_{z\pm} = C_\pm|1 - T/T_c|^{-1.19(2)}$ with amplitudes $C_+ = 1.4(1) \times 10^{-4}$ and $C_- = 0.7(1) \times 10^{-4}$, above and below T_C, respectively, and for the spontaneous magnetization, $M_s = 3.6$ kOe $(1 - T/T_C)^{0.39(1)}$. These findings are in good accordance with independent

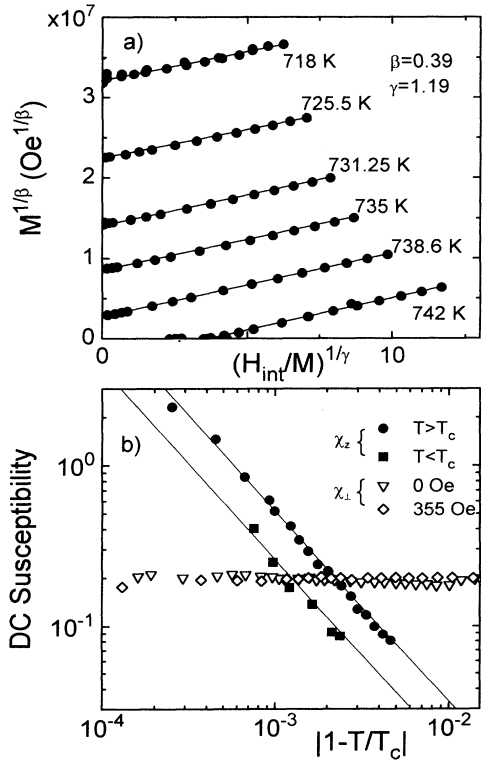

FIG. 5. Critical behavior (a) of the longitudinal magnetization and (b) of the longitudinal and transverse internal susceptibilities near T_C.

recent results for $SrFe_{12}O_{19}$.[13] The longitudinal susceptibilities agree also with the zero-frequency limit of $\chi_d(\omega)$ [see Eq. (2.1)] using $\chi_z^{-1} = \chi_d^{-1}(\omega = 0) - N_z$, shown in Fig. 5(b). Hence we can conclude that the second, fast process in Eq. (2.1) arises from the spin relaxation in the homogeneous phase in the domains, supporting the earlier conclusion that the slow one arises from the relaxational wall dynamics. The transverse static susceptibilities also shown in Fig. 5(b) were determined by orientating the sample with the easy axis perpendicular to the symmetry axis of the pickup coils. We obtained $\chi_\perp = 0.20(2)$ independent of temperature and field.

III. WALL DYNAMICS: GENERAL CONSIDERATIONS

A. Kinetic coefficient

The basic features of the domain-wall relaxation in zero as well as in finite magnetic fields will be discussed in terms of the kinetic Onsager coefficient L_w which according to previous work[3] describes the magnetization change due to the wall motion in response to the instantaneous internal field, $\dot{M}_w(t) = L_w H_z(t)$, and hence reflects the intrinsic wall dynamics. To determine L_w from the measured relaxation rates Γ_w, the contribution of the magnetization within the domains to the total magnetization process has to be considered. According to Ref. 3, the instantaneous internal field driving the domain walls is reduced by the action of the demagnetizing field arising from the fast intradomain magnetization response, $M_d(t) = \chi_d H_z(t)$, and one measures the relaxation rate

$$\Gamma_w = \frac{L_w}{\chi_w}\left(1 - \frac{\chi_d}{\chi_w}\right). \tag{3.1}$$

At low temperatures, where $\chi_d \ll \chi_w$, the correction factor due to the intradomain effect can be ignored. Equation (3.1) also shows that considering L_w instead of Γ_w eliminates the thermodynamic effect of the bulk susceptibility on the wall dynamics, and the mesoscopic and microscopic effects on the wall dynamics are retained in L_w.

For small driving fields $H_z(t)$, the kinetic coefficient is directly related[3,7] to the well-known wall mobility, μ_w, which depends only on the properties of the DW's:

$$L_w(T, \mathbf{H}, D) = \frac{2M_s(T)\sqrt{1 - (\chi_\perp H_y M_s)^2}}{d(T, \mathbf{H}, D)}\mu_w(T, H_y). \tag{3.2}$$

Here d represents the domain period which results from a minimization of the total magnetic energy of the sample ellipsoid of thickness D along the (principal) c direction subjected to a magnetic field H_z applied parallel to **c**.

B. Wall mobility

In the consideration of the DW dynamics in uniaxial ferromagnets at finite temperatures and where the phase

transition from Bloch to linear walls occurs one has to take into account both transverse and longitudinal relaxation of the magnetization. An appropriate deterministic equation of motion for the magnetization at elevated temperatures is the so-called Landau-Lifshitz-Bloch (LLB) equation of motion[7,8] microscopically derived based on the molecular field approximation. At both low and high temperatures the well-known Landau-Lifschitz and Bloch equations are recovered. In the case of ordered magnetic materials, the LLB equation coincides with the phenomenological equation by Baryakhtar.[14] For the calculation of the DW mobility in the linear regime ($v \propto \Delta H_z$) with the help of the LLB equation one has to know the *static* magnetization distribution in a wall. The general expression for μ_w in a uniaxial ferromagnet[8] including the case of the transverse field in the DW plane (see also Ref. 15) can be represented in the form

$$\mu_w^{-1} = \mu_1^{-1} + \mu_2^{-1}, \tag{3.3}$$

where μ_1^{-1} and μ_2^{-1} are the contributions of the longitudinal and transverse relaxation mechanisms to the DW damping given by the integrals over the static magnetization profile $\mathbf{m}(x)$:

$$\mu_1 = 2\gamma\alpha_z m_z(\infty)\left[\int_{-\infty}^{\infty} dx \frac{1}{4m^2}\left(\frac{dm^2}{dx}\right)^2\right]^{-1}, \tag{3.4}$$

$$\mu_2 = 2\gamma\alpha_\perp m_z(\infty)\left\{\int_{-\infty}^{\infty} dx \frac{1}{1+(m/\alpha_\perp)^2} \times\left[\left(\frac{dm}{dx}\right)^2 - \frac{1}{4m^2}\left(\frac{dm^2}{dx}\right)^2\right]\right\}^{-1}. \tag{3.5}$$

Here the wall magnetization has been normalized to M_s, $\mathbf{m}(x) = \mathbf{M}(x)/M_s$, and the in-plane transverse field H_y to the anisotropy field $h_y = H_y/H_A = (H_A/M_s)\chi_\perp$. For $h_y < 1$, the magnetization in the adjacent domains is given by

$$m_y(\pm\infty) = h_y, \qquad m_z(\pm\infty) = \pm\sqrt{1-h_y^2}. \tag{3.6}$$

The so-called Gilbert-damping parameters have been denoted by $\alpha_z = L_z/\gamma M_s$ and $\alpha_\perp = L_\perp/\gamma M_s$. Note that due to $m_x = 0$ in a conventional BW, the H_x component of the applied field does not couple to the wall magnetization. Since the H_z component is excluded from the bulk of the sample by the demagnetizing fields extending from the surface, only H_y can have an effect on the wall mobility.

The DW magnetization profile $\mathbf{m}(x)$ is determined by minimizing the free energy of a planar wall in a uniaxial ferromagnet which reads in the MFA

$$F_w = M_s^2 \int dxdydz\left[\left(\frac{\nabla\mathbf{m}}{q_d}\right)^2 + \frac{(m_y-h_y)^2}{\chi_\perp} + \frac{(1-m^2)^2}{4\chi_z}\right], \tag{3.7}$$

where q_d is the dipolar wave number determined by the ratio between dipolar energy and the second moment of the exchanges or experimentally[16] by $q_d^2 = \chi_z/\xi_z^2$. The minimization leads to the differential equation

$$\frac{1}{q_d^2}\frac{d^2\mathbf{m}}{dx^2} = -\frac{1-m^2}{2\chi_z}\mathbf{m} + \frac{m_y-h_y}{\chi_\perp}\mathbf{e}_y. \tag{3.8}$$

Analytical solutions of Eq. (3.8) do not exist, and from the solvable special cases we mention the case of zero transverse field,

$$m_y(x) = \frac{\rho}{\cosh(x/\delta)}, \quad m_z(x) = -\tanh(x/\delta), \tag{3.9}$$

where the shape and the width are given by $\rho = m_B^{\mathrm{MF}}(\tau)$ [see Eq. (1.1)] and

$$\begin{aligned}\delta(\tau \le 1, h_y = 0) &= \sqrt{\chi_\perp}/q_d \equiv \delta_B,\\ \delta(\tau \ge 1, h_y = 0) &= 2\sqrt{\chi_z}/q_d \equiv \delta_L.\end{aligned} \tag{3.10}$$

As anticipated in the Introduction, the temperature T_{MF}^* defined by the condition

$$\tau(T_{\mathrm{MF}}^*) = \frac{4\chi_z(T_{\mathrm{MF}}^*)}{\chi_\perp} = 1 \tag{3.11}$$

represents the critical point for the structural transition of the DW from linear to elliptic shape, $m_y^2/\rho^2 + m_z^2 = 1$. The latter passes to the circular Bloch shape when $\tau \ll 1$, and according to Eq. (1.1) this limit implies $m_B(\tau) = 1$, but necessarily not $T \ll T_C$.

In the presence of an applied field $\mathbf{H}$, where in the MFA only H_y affects the wall mobility, we search for the DW profile using the trial function

$$\begin{aligned}m_y(x) &= m_y(\infty)\frac{\cosh(x/\delta) + \rho/h_y}{\cosh(x/\delta) + h_y},\\ m_z(x) &= m_z(\infty)\frac{\sinh(x/\delta)}{\cosh(x/\delta) + h_y}.\end{aligned} \tag{3.12}$$

This ansatz satisfies the boundary conditions (3.6) and reproduces the solutions (3.10) in the limit $h_y \to 0$. For this general case, the trial function is inserted into the free energy F_w to yield after integration over x the DW energy per unit area $\sigma_w(\delta, \rho, \tau, h_y)$. Minimizing σ_w at fixed ρ with respect to the DW width δ we find

$$\delta^2(\tau, h_y, \rho) = \delta_B^2\tau\frac{aI - \bar\rho(2a-\bar\rho)J}{A + \tau(a-\bar\rho)^2 I}, \tag{3.13}$$

with $a = 1 - h_y^2$, $\bar\rho = 1 - \rho$, and

$$A = (\bar\rho^2/a)\left[(4a - \bar\rho^2)I - (2a-\bar\rho)(2a+5\bar\rho)J\right], \tag{3.14}$$

and the field-dependent functions

$$I(h) = \frac{1}{1-h^2}\left(1 - \frac{h}{\sqrt{1-h^2}}\arctan\frac{\sqrt{1-h^2}}{h}\right), \tag{3.15}$$

$$J(h) = \frac{1}{2(1-h^2)^2}\left(\frac{2}{3}+\frac{1}{3}h^2 - \frac{h}{\sqrt{1-h^2}}\arctan\frac{\sqrt{1-h^2}}{h}\right). \quad (3.16)$$

Using this result the specific wall energy can be represented in the form

$$\sigma_w = \frac{2M_s^2}{\chi_\perp}\frac{\delta_B}{\sqrt{\tau}}\sqrt{[aI-\bar{\rho}(2a-\bar{\rho})J][A+\tau(a-\bar{\rho})^2 I]}. \quad (3.17)$$

Further minimization of σ_w with respect to the shape parameter ρ yields an implicit equation for ρ,

$$\sum_{n=0}^{5} Q_n(\tau, h_y)(1-\rho)^n = 0, \quad (3.18)$$

the coefficients of which are defined as

$$\begin{aligned} Q_5 &= (6/a)J(5J-I), \\ Q_4 &= -10J(9J-I), \\ Q_3 &= 4I(9I-J)+48aJ^2+4\tau IJ, \\ Q_2 &= -12aJ(4I-2aJ+\tau I), \\ Q_1 &= 8aI(I-aJ)+2\tau aI^2+10\tau a^2 IJ, \\ Q_0 &= -2\tau a^2 I(I+aJ). \end{aligned} \quad (3.19)$$

Detailed analyses[17] show that to good accuracy these results also reproduce the perturbative solutions of Eq. (3.8) available in the limits $\tau \gg 1$, $\tau \ll 1$, and for $h \ll 1$ in the LW region.

IV. DISCUSSION OF WALL RELAXATION

In this section, we will discuss the experimental results on the influence of temperature, sample thickness, and longitudinal and transverse applied fields on the kinetic coefficient of the walls. This discussion will be based on the kinetic LLB theory presented in the preceding section. For this purpose, we will consider separately the effects on L_w arising from changes (i) of the domain structure induced by longitudinal fields and varying sample thickness D, (ii) of the temperature which causes the structural transition of the DW's, and (iii) of the transverse fields polarizing the order parameter of the BW's.

A. Effects of size and longitudinal fields

The domain structure of the hexaferrite $BaFe_{12}O_{19}$ was investigated by Kooy and Enz,[18] who using the Faraday effect observed the stripe structure for applied fields below $H_z = N_z M_s$ and calculated the magnetostatic energy of this domain structure. From their result Rajchenbach[19] derived the field dependence of the domain period

$$d(T, H_z, D) = d(T, 0, D)G(h_z), \quad (4.1)$$

where the factor

$$G(h_z) = \left(0.95\sum_{n=1}^{\infty}\frac{1}{n^3}\sin^2\left[\frac{n\pi}{2}(1+h_z)\right]\right)^{1/2}$$

increases with the normalized field $h_z = H_z/N_z M_s$. At zero field, the period can be determined from the minimum of the wall and surface energies. The results[3] for stripe[20] and for branched surface domains can be represented in the form

$$d(T, 0, D) \approx 2\frac{D^\eta q_d^{\eta-1}}{(\delta(T)q_d)^{1-\eta}}, \quad (4.2)$$

with $\eta = 1/2$ and $2/3$ for the striped and branched cases, respectively, where δ is the width of the DW.

The domain profile $\mathbf{m}(x)$ is known within the MFA for zero transverse field, Eqs. (3.9), (3.10). Using this profile and calculating the wall mobilities from the LLB results Eqs. (3.3)–(3.5), one obtains, for the kinetic coefficient from Eq. (3.2),

$$L_w(T, h_z, D) = \frac{(\delta(T)q_d)^{2-\eta}}{(Dq_d)^\eta}L_z \times \frac{G(h_z)}{f_1(m_B)+(L_z/L_\perp)f_2(m_B)}, \quad (4.3)$$

where

$$f_1(m_B) = \frac{2}{3}+\frac{1}{3}m_B^2 - \frac{m_B}{\sqrt{1-m_B^2}}\arctan\frac{\sqrt{1-m_B^2}}{m_B}, \quad (4.4)$$

$$f_2(m_B) = \frac{m_B}{\sqrt{1-m_B^2}}\arctan\frac{\sqrt{1-m_B^2}}{m_B} - \frac{m_B^2}{\sqrt{(1-m_B^2)(m_B^2+\alpha_\perp^2)}} \times \arctan\sqrt{\frac{1-m_B^2}{m_B^2+\alpha_\perp^2}}. \quad (4.5)$$

Let us first consider the effect of D. Figure 6(a) demonstrates that the kinetic coefficient L_w measured in zero applied field scales indeed with the thicknesses of the ellipsoids between 0.1 mm and 2 mm along the c direction investigated here,

$$L_w(T, 0, D) = L_w(T, 0, D_0)\left(\frac{D}{D_0}\right)^\eta. \quad (4.6)$$

The exponent of this size scaling, $\eta = 0.61(4)$, is closer to $\eta = 2/3$ predicted by Eq. (4.3) for the case of domain branching near the surface than to $\eta = 1/2$ for the Kittel domains.[20] Perhaps our intermediate value is thus associated with the wavy surface domain structure discovered recently on $BaFe_{12}O_{19}$ by magnetic force microscopy.[21] The same argument was used by Kaczér and Gemperle[22] to explain $\eta = 0.63$ obtained from investigations of $d(D)$ on Pb hexaferrite. A very similar exponent η was found

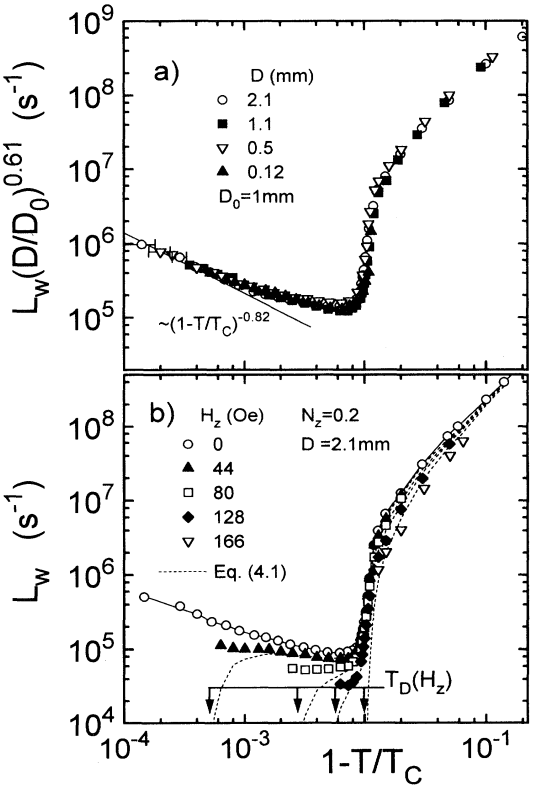

FIG. 6. Temperature variation of the kinetic coefficient of wall relaxation (a) in zero applied field, scaled to the sample length D along the easy axis, and (b) in fields applied parallel to the easy axis. $T_D(H_z)$ are the transition temperatures from the domain to the homogeneous state; the solid curve through $H_z = 0$ represents a smooth spline function; dashed curves are fits to Eq. (4.7).

for the kinetic coefficient of the linear walls in the uniaxial ferromagnet $LiTbF_4$,[4] with $T_C = 2.87$ K, and so we conclude that the size effect is of purely magnetostatic origin and does not interfere with thermal fluctuations.

The effect of magnetic fields H_z applied parallel to the measuring direction, i.e., to the easy c direction of one sample ellipsoid, is shown in Fig. 6b. It turns out that the kinetic coefficient generally decreases with H_z as predicted by Eq. (4.3), which we rewrite for this comparision in the form

$$L_w(T, H_z, D) = L_w(T, 0, D)G(h_z). \qquad (4.7)$$

In Fig. 6(b), $L_w(T, 0, D)$ is represented by a spline function through the zero-field data as a solid curve. Inserting this function and the field factor $G(h_z)$ of Eq. (4.1) into Eq. (4.7) one obtains field-dependent kinetic coefficients as indicated by the dotted lines. Obviously, for small values of the normalized field, $h_z = H_z/N_z M_s(T) \ll 1$, the data follow rather nicely the predicted curves; however, approaching the stability limit of the domains $h_z(T_D) = 1$ the measured values do not display a downward curvature. Such deviations have also been realized on the low-temperature uniaxial ferromagnets $GdCl_3$ (Ref. 3) and $LiTbF_4$ (Ref. 23) and were qualitatively attributed to an increasingly inhomogeneous magnetic structure, because near T_D the domain period d reaches the order of the sample thickness D. Then the demagnetizing fields extending from the surface poles penetrate deeply into the sample and into the walls, which increases the magnetic inhomogenity and gives rise to a softer domain structure. Empirically, this may be characterized by a larger effective wall parameter, $\delta(T, H_z)$, which according to Eq. (3.1) leads to a larger kinetic coefficient. It is perhaps interesting to note that even for $h_z \gtrsim 1$, there are some remnants of wall dynamics which we attribute to DW fluctuations in the homogeneous phase.

We note that near $T_D(H_z)$ the differences between the L_w data and the micromagnetic calculation become greater with increasing field, i.e., with decreasing transition temperatures $T_D(H_z)$. This contrasts to the case of the uniaxial ferromagnets with low T_C's,[3,23] where this difference decreased. We attribute this observation to the fact that, in the hexaferrite, $T_D(H_z)$ approaches the stability limit of the linear-wall structure at T^* whereas, due to the larger spin susceptiblity $\chi_z(T)$ in the low-T_C ferromagnets, T^* was not reached by $T_D(H_z)$. Here we conclude that for $T_D(H_z) \to T^*$ the wall fluctuations near T^* are further enhanced due to the instability of the domain structure itself.

B. Temperature variation

In Fig. 7(a), the data measured on one sample ($D =$ 2.1 mm) in zero applied field are shown and compared

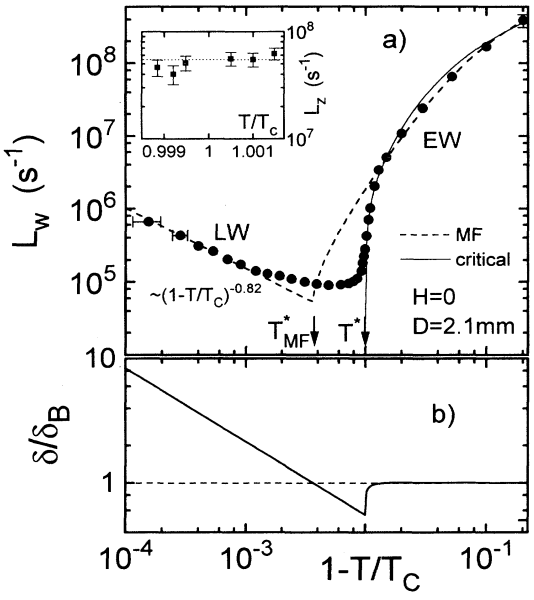

FIG. 7. (a) Kinetic coefficient of wall relaxation in zero field showing the crossover from linear walls (LW's) near T_C to elliptic walls (EW's) below T^* to Bloch walls (BW's) at low temperatures. The dashed curve is a fit to Eq. (3.2), using the mean-field prediction for the DW order parameter m_B, Eq. (1.1), and for the width, Eq. (3.10). The inset demonstrates the noncritical behavior of the kinetic coefficient L_z of the homogeneous phase. Effects of 2D Ising fluctuations on m_B and the wall thickness δ are shown in (b).

to a calculation using Eqs. (4.3)–(4.5) in which the MFA results for the order parameter, $m_B = m_B^{\rm MF}$, and transition temperature, $T^*_{\rm MF}$, following from Eqs. (1.1) and (1.2) have been inserted. We emphasize that the significant suppression of the minimum in L_w occurring at $T^* < T^*_{\rm MF}$ is responsible for the strong differences between the MFA prediction and the data in this transition region. On the other hand, there is convincing agreement outside this region, i.e., for $\tau > \tau^* = \tau(T^*) = 0.27$,[6] where the LW's are stable, and for $\tau < \tau^*$, where the EW's exist. In each regime, we have adjusted one of the two relaxation parameters L_z and $L_\perp$ contained in Eq. (4.3).

For linear walls with $\delta = \delta_L$, $m_B = 0$, and $f_2(0) = 0$, one finds from Eq. (4.3)

$$L_w(T > T^*, 0, D) = \frac{2}{3} L_z \frac{[\delta_L(T) q_d]^{2-\eta}}{(D q_d)^\eta}, \tag{4.8}$$

which has to be compared to the critical speeding up measured near T_C, $L_w(T) = L_w(0)(1-T/T_C)^{-z}$. Taking, from Eq. (3.10), $\delta_L^2(T) = 4\chi_z(T)/q_d^2$ and the measured susceptibility, $\chi_z = C_-(1-T/T_C)^{-\gamma}$ [see Fig. 5(b)], one finds for the critical exponent $z = (1-\eta/2)\gamma = 0.82(4)$.[24] According to Fig. 6(a) this value is consistent with the data away from $T^*_{\rm MF}$, so that we can conclude that the kinetic coefficient of the spin-lattice relaxation L_z does not depend on temperature. Such uncritical behavior of L_z is typical of uniaxial systems which display pure relaxational dynamics, and the associated thermodynamic slowing down $\Gamma_d = L_z/\chi_z$ (type A in the classification of Ref. 25) has frequently been realized in uniaxial ferromagnets.[3,4,26] These studies also revealed that L_z is determined by the relaxation rate of the homogeneous phase. For $SrFe_{12}O_{19}$, one finds from $\Gamma_d = L_z/\chi_d$ measured above and below T_C, $L_z = 55(10) \times 10^6$ s^{-1}, depicted by the inset to Fig. 7(a). Using this number, we find that the measured coefficient of the speeding up, $L_w(0) = 530$ s^{-1}, is reproduced by Eq. (4.8) if we take $q_d = 0.01$ nm^{-1} as the dipolar wave number. This value for q_d proves to be quite reasonable when we estimate the range of the ordering interaction,[27] $r_0 \approx (\lambda_c/T_C)^{1/2}/q_d$. Using the bare susceptibility at T_C for $SrFe_{12}O_{19}$, $\lambda_c/T_C = 10^{-4}$, we find $r_0 = 1$ nm which, considering the large ferrimagnetic unit cell,[28] can be accepted. Hence we conclude that, similar as for the uniaxial ferromagnet $GdCl_3$,[26] the critical speeding up of L_w for LW's in $SrFe_{12}O_{19}$ has almost quantitatively been explained.

In the other limit of elliptical walls, present at lower temperatures where $\tau \to 0$ and $m_B \to 1$, one obtains in the denominator of Eq. (4.3), $f_1(m_B) + \alpha_z\alpha_\perp$ for the present case of small Gilbert parameters, $\alpha_z, \alpha_\perp \ll 1$. Fitting the low-temperature data to this expression, we find $L_z L_\perp = 7.8 \times 10^{16}$ s^{-2} which implies $L_\perp = 1.3 \times 10^9$ s^{-1}, in good accordance with $L_\perp = \chi_\perp/T_2 = 0.9 \times 10^9$ s^{-1} determined from the ferrimagnetic resonance linewidth for the closely related material, $BaFe_{12}O_{19}$.[29] Inserting $L_\perp$ into Eq. (4.3) the data are well described except for temperatures near the wall transition.

In the absence of theoretical work considering the influence of order parameter fluctuations on both the wall profile $\mathbf{m}(x)$ and the dynamics of $\mathbf{m}$, previous work[6] proposed to allow the BW order parameter to vary in terms of the general power law, $m_B(\tau) = (1-\tau/\tau^*)^\beta$ [Eq. (1.3)]. In fact, rather convincing agreement with the data was achieved using the significantly lower transition temperature $\tau^* = \tau(T^*) = 0.27$ and $\beta = 0.08(1)$ for the critical exponent. Since β was not only much smaller than the MFA value, $\beta = 1/2$, but even smaller than that of the two-dimensional Ising model, $\beta = 1/8$, proposed by Lawrie and Lowe,[10] it was conjectured that not all aspects of the fluctuations have been taken into account. In particular, out-of-DW-plane fluctuations and dynamical critical effects not accounted for in the LLB equations have been suggested, which, however, are far too complicated as to be considered here. Instead, we perform here a smaller step in order to improve the approach of Ref. 6: We do not fix any longer the DW width below T^* to $\delta(\tau < 1) = \delta_B$, Eq. (3.10), but we use the variational result for δ, Eq. (3.13), with $\rho(h_y = 0) = m_B$,

$$\delta^2(\tau) = \delta_B^2 \tau \frac{1 + m_B^2/2}{(1-m_B^2)^2 + (3/2)\tau m_B^2}, \tag{4.9}$$

which implies a temperature variation of δ also below T^*. In fact, inserting this expression into Eq. (4.3) to fit L_w to the data below T^* we obtain $\beta = 0.11(2)$ as represented by the solid line in Fig. 7(a). The corresponding temperature variation of δ is shown in Fig. 7(b) which reveals that δ_B is suppressed by the factor τ^* due to reduction of the transition temperature from $\tau^*_{\rm MF} = 1$ to $\tau^* = 0.27$ by the fluctuations. The most interesting consequence of the present approach is that the critical exponent of the BW order parameter moved towards the two-dimensional Ising value, $\beta = 0.125$. This provides more evidence for the critical fluctuations occuring very close to τ^* where the range of their correlations ξ_B are much larger than δ_B. Using the dipolar wave number of $SrFe_{12}O_{19}$ determined before, we find $\delta_B = \sqrt{\chi_\perp}/q_d = 40$ nm as an estimate for the crossover to three-dimensional behavior.

C. Effects of transverse fields

The speeding up of the DW relaxation rate Γ_w in the presence of fields $H_\perp$ applied perpendicular to the easy c axis has been illustrated already in Fig. 4 and contrasted to the effect of longitudinal fields. Here we will discuss the results for the wall kinetic coefficients displayed in Fig. 8, the most interesting phenomena of which are the following: (i) The minimum of L_w becomes flatter and is shifted towards higher temperatures with increasing $H_\perp$, (ii) the effect of $H_\perp$ on L_w is largest near the minima and becomes independent of T above the minima, and (iii) immediately below T^*, $H_\perp$ exerts only a weak effect on L_w. Feature (iii) is expected from the fact that, below T^*, m_B rapidly saturates already for $H_\perp = 0$ so that the transverse field cannot polarize m_B very much. On the other hand, similarly as for the field dependence of the susceptibility of a bulk ferromagnet, very small fields have the maximum effect on m_B at T^*, while with

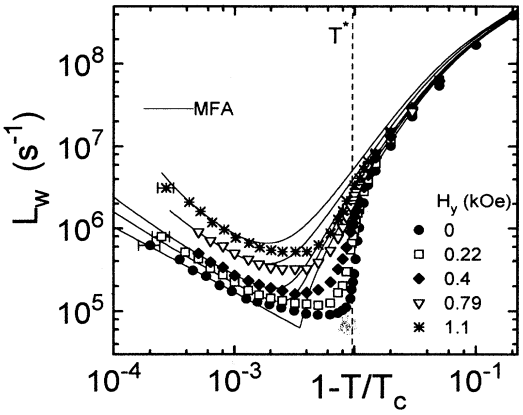

FIG. 8. Temperature variation of the wall kinetic coefficient in fields perpendicular to the easy c axis. Solid curves are fits to Eq. (3.2) based on the mean-field solutions for the wall magnetization profile, Eqs. (3.12)–(3.18).

increasing $H_\perp$ the susceptibility $dm_B/dH_\perp$ attains the maximum at temperatures above T^*. Taking this into account and recalling that the wall mobility μ_w and hence L_w increase with $m_B(T, H_y)$, features (i) and (ii) can be understood on a qualitative basis.

In order to gain a deeper insight into this polarization process, we determined the wall profile in the MFA from the variational ansatz, Eq. (3.12), using the result Eq. (3.13) for ρ. Since the applied field suppresses fluctuations, we can expect that the MFA approach will improve with increasing $H_\perp$. Indeed, the comparison between measured and calculated wall kinetic coefficients in Fig. 8 shows that the overall difference is smallest for the highest field of 1.1 kOe and also for low temperatures, $T < T^*$, but the MFA clearly fails in the critical regime of the disordered BW phase, i.e., between $T^*_{\rm MF}$ and T^*. Note that the MFA calculations do not employ any additional parameter, except for the fact that we have to assume $H_y = \frac{1}{2}H_\perp$ for *all* applied fields $H_\perp$ to obtain agreement in the MF regime. Such a reduction of the effective polarizing field is not implausible because in a real sample the orientation of the BW's and of their order parameter is randomly distributed while the present treatment applies to planar walls, aligned parallel to $H_\perp$. We do not examine this feature in more detail, mainly because we have no detailed information on the real domain structure in the bulk.

Let us finally point out that we also made no attempt here to improve the agreement between MFA and the data, mainly for two reasons: (i) Below the transition temperature the differences are small, and (ii) above T^* the fluctuations of the order parameter and of the wall thickness are very large, and a realistic approach taking into account their effect on both the statics and the dynamics of the walls is not yet available, not even for a zero transverse field.

V. CONCLUSIONS

The rather dramatic slowing down of the domain-wall relaxation in Sr hexaferrite observed here when approaching the temperature $T^* = 0.99\,T_C$ from below can rather convincingly be ascribed to the decrease of the order parameter of the Bloch walls, $m_B = M_y(x = 0)/M_s$, i.e., the in-plane magnetization in the center of the wall. Our analysis based on the kinetic Landau-Lifschitz-Bloch equations and on an extended mean-field approximation for the wall profile below T^* reveals that m_B rapidly vanishes near T^* in close correspondence to the order parameter of the two dimensional Ising model. Taking for granted the concept of a one-component order parameter proposed by Bulaevski and Ginzburg[1] for the BW, this behavior is plausible for the present wall structural phase transition, if the wall can be considered as planar and two dimensional close to T^*, where the correlation length of m_B exceeds the thickness of the wall. Above T^*, the wall relaxation speeds up towards the Curie temperature in terms of a power law, which, in accordance with previous results in other materials,[3,4] is attributed to relaxational dynamics of linear walls. Their width is determined by the correlation length of the bulk magnetization M_z diverging at T_C.

By adopting the conventional magnetostatic results for the domain structure, we were able to describe also quantitatively the variation of the relaxation rates with sample size and longitudinal applied fields, and even their absolute magnitude could be explained using intrinsic spin-lattice and spin-spin relaxation constants known from independent measurements. Further support for the validity of the MFA to the domain-wall structure and the LLB kinetics used here was gained from the successful explanation of the speeding up of the relaxation rates induced by magnetic fields applied transverse to the c axis.

In the critical regime on the disordered side, i.e., for $T \gtrsim T^*$, however, significant deviations remained between the predictions of the kinetic LLB theory and the measured temperature and field variations of the wall relaxation rate. Here severe fluctuations of the BW order parameter can be expected, which presumably control both the width and the dynamics of the wall in a way that cannot be discussed based on the approaches introduced here. This will require much more extensive theoretical treatments of the critical statics and dynamics of the wall magnetization $\mathbf{M}(x)$ near T^*. On the experimental side, investigations of DW dynamics in ferro- and ferrimagnets with stronger anisotropy would be of interest, because in this case [see Eq. (1.2)] T^*/T_C decreases to lower values and the critical phenomena near the wall reconstruction at T^* do not interfere with those associated with the bulk transition.

ACKNOWLEDGMENTS

The authors are indebted to L. Jahn (Dresden), K.A. Hempel, and D. Bonnenberg (Aachen) for providing the single crystals used here and to Hartwig Schmidt and D. Fay (Hamburg) for interesting comments.

[1] L.N. Bulaevskii and V.L. Ginzburg, Sov. Phys. JETP **18**, 530 (1964).
[2] L.N. Bulaevskii and V.L. Ginzburg, JETP Lett. **11**, 272 (1970).
[3] M. Grahl and J. Kötzler, Z. Phys. B **75**, 527 (1989).
[4] J. Kötzler, M. Grahl, I. Sessler, and J. Ferré, Phys. Rev. Lett. **64**, 2446 (1990).
[5] J. Kötzler, M. Hartl, and L. Jahn, J. Appl. Phys. **73**, 6263 (1993).
[6] J. Kötzler, D.A. Garanin, M. Hartl, and L. Jahn, Phys. Rev. Lett. **71**, 177 (1993).
[7] L.V. Panina, D.A. Garanin, and I.G. Rusavin, IEEE Trans. Magn. **MAG-26**, 2816 (1990).
[8] D.A. Garanin, Physica A **172**, 470 (1991); **178**, 467 (1991).
[9] L. Landau and E. Lifshitz, Z. Phys. Sowjetunion **8**, 153 (1935).
[10] I.D. Lawrie and M.J. Lowe, J. Phys. A **14**, 981 (1981).
[11] L. Jahn and H.G. Müller, Phys. Status Solidi A **35**, 723 (1969).
[12] J. Kötzler, D. Görlitz, M. Hartl, and Chr. Marx, IEEE Trans. Magn. **MAG-30**, 828 (1994).
[13] H. Gerth and H. Kronmüller, J. Magn. Magn. Mater. **130**, 73 (1994).
[14] V.G. Baryakhtar, Sov. Phys. JEPT **64**, 857 (1984); Sov. Phys. Solid State **29**, 754 (1987).
[15] B.A. Ivanov and K.A. Safariyan, Sov. Phys. Solid State **32**, 2034 (1990).
[16] J. Kötzler, J. Magn. Magn. Mater. **54-57**, 649 (1986).
[17] D.A. Garanin (unpublished).
[18] C. Kooy and U. Enz, Philips Res. Rep. **15**, 7 (1960).
[19] J. Rajchenbach, J. Phys. C **21**, L447 (1988).
[20] C. Kittel and J.K. Galt, Solid State Phys. **3**, 437 (1956).
[21] A. Wadas, H.J. Hug, and H.-J. Güntherodt, Appl. Phys. Lett. **61**, 357 (1992).
[22] J. Kaczér and R. Gemperle, Czech. J. Phys. B **10**, 505 (1960).
[23] M. Grahl, Ph.D. thesis, Hamburg University, 1990.
[24] Due to the availability of much more data and an accurate value for T_C, the value quoted here is more precise than $z = 0.89$, for which no error margin could be determined in Ref. 6.
[25] P.C. Hohenberg and B.I. Halperin, Rev. Mod. Phys. **49**, 435 (1977).
[26] M. Grahl, J. Kötzler, and I. Sessler, J. Magn. Magn. Mater. **90&91**, 187 (1990).
[27] S.V. Maleev, Soc. Sci. Rev. A Phys. **8**, 323 (1987).
[28] J. Smit and H.P.J. Wijn, *Ferrites* (Philips' Technical Library, Eindhoven, The Netherlands, 1959), Chap. IX.
[29] P. Grohs, K.A. Hempel, and H.J. Rüschenbaum, J. Magn. Magn. Mater. **54-57**, 1633 (1986).